ELSEVIER

Journal of Power Sources 54 (1995) 346–351

JOURNAL OF POWER SOURCES

Electrochemical insertion of lithium, sodium, and magnesium in molybdenum(VI) oxide

M.E. Spahr [a], P. Novák [a,*], O. Haas [a], R. Nesper [b]

[a] *Paul Scherrer Institute, Electrochemistry Section, 5232 Villigen PSI, Switzerland*

[b] *Swiss Federal Institute of Technology (ETH), Laboratory for Inorganic Chemistry, 8092 Zurich, Switzerland*

Abstract

The electrochemical insertion of divalent magnesium cations into orthorhombic molybdenum(VI) oxide was studied with regard to their use as electroactive species in ion-transfer battery systems and compared to the insertion of Li^+ and Na^+. Specific charges of up to 300 and 240 Ah kg^{-1} were obtained in organic, propylene carbonate-based electrolytes for the lithium and sodium insertion, respectively, in the first reduction half-cycle. Reversible Mg^{2+} insertion could be demonstrated in a room temperature molten salt electrolyte consisting of 3 wt.% $MgCl_2$, 41 wt.% 1-ethyl-3-methylimidazolium chloride, and 56 wt.% $AlCl_3$. Specific charges of up to 160 Ah kg^{-1} were obtained with MoO_3 in the first reduction half-cycle. The Mg^{2+} insertion process can be enhanced using an organic electrolyte with traces of H_2O. In 1 M $Mg(ClO_4)_2$/acetonitrile with 3 mol% of H_2O, specific charges of up to 210 Ah kg^{-1} were measured in the first reduction.

Keywords: Molybdenum oxide; Lithium; Sodium; Magnesium; Insertion

1. Introduction

Unlike the cases of lithium and sodium, the chemical and electrochemical insertion of divalent cations in transition metal oxides and sulfides has been studied only in a limited number of investigations. Especially the insertion of magnesium is of particular theoretical and practical interest, both because of the similar ion size of monovalent lithium and divalent magnesium cations, which may lead, from a steric point of view, to an analogous insertion electrochemistry, and because of a prospective application in ion-transfer battery systems. The equivalent weight of magnesium (12 g per Faraday) is not much higher than that of lithium (7 g per Faraday) but significantly lower than that of sodium (23 g per Faraday). Moreover, in ion-transfer batteries, magnesium might be advantageous to lithium due to its natural abundance, relatively low price, and higher expected safety. However, the insertion chemistry and electrochemistry of magnesium show some special features [1–9], and their understanding seems to be still in the beginning stages.

Orthorhombic molybdenum trioxide is known to be a typical host for many monovalent and multivalent cations that are inserted chemically or electrochemically. Since the electrochemical insertion of lithium in MoO_3 is reversible, the application of this material in secondary lithium batteries and electrochromic devices has been suggested [10–13].

The redox mechanism for the lithium insertion in MoO_3 seems to be well understood [14]. The insertion suitability of MoO_3 is derived from its unique layer structure that is shown in Fig. 1 [15]. Edge- and corner-sharing [MoO_6] octahedra build up double layers. These

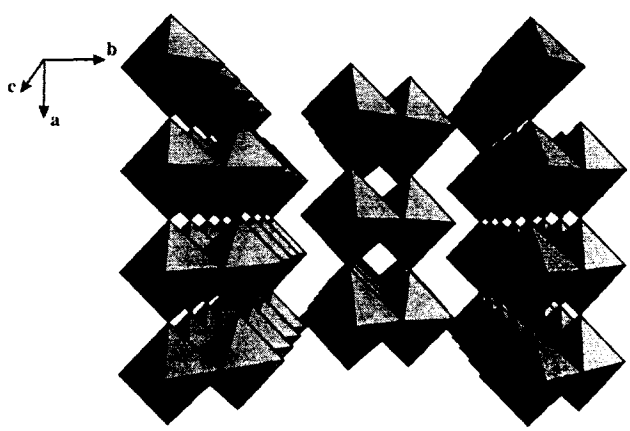

Fig. 1. Crystal structure of orthorhombic MoO_3 [15].

* Corresponding author.

SSDI 0378-7753(94)02099-O

layer planes characterized by strong covalent bonds are held together by weak van der Waals attraction forces. The interlayer distance has been determined to be 6.929 Å [15]. The reversible electrochemical behaviour of the MoO_3 electrodes can be explained on the grounds of topotactic redox phenomena. The transition metal oxide layers are retained as two-dimensional matrix units during the insertion and de-insertion process. The electrode process could be described according to:

$$MoO_3 + xLi^+ + xe^- \longleftrightarrow Li_xMoO_3 \quad (1)$$

Relatively low specific energies of the Li/MoO_3 couple and poor cycling stability of the oxide are recognized drawbacks of MoO_3 as an electrode material in lithium ion-transfer batteries. Nevertheless, its host properties could be conveniently used for electrochemical insertion experiments of divalent magnesium cations from non-aqueous electrolytes. Gregory et al. [4] listed molybdenum trioxide as one of the oxides being capable of Mg^{2+} insertion. From *chemical* insertion tests in a solution of dibutylmagnesium in heptane as insertion reagent, a specific charge of about 140 Ah kg^{-1} corresponding to a stoichiometry of $Mg_{0.5}MoO_3$ was estimated [4]. However, another group measured a much lower magnesium content after chemical insertion, also using the dibutylmagnesium/heptane solution, namely $Mg_{0.05}MoO_3$ [1]. The aim of this paper is to investigate the *electrochemical* insertion of magnesium in MoO_3 from non-aqueous electrolytes; the Mg^{2+}-insertion process and the specific charges attained in electrochemical experiments are compared with data from the appropriate lithium and sodium systems.

2. Experimental

Insertion experiments were carried out in gas-tight sealed laboratory cells with a three-electrode arrangement in which the working and counter electrodes were slightly mechanically pressed together against a glass-fibre separator soaked with an electrolyte solution. The working electrodes had a geometrical area of 1.3 cm^2 and contained approximately 10 mg of orthorhombic MoO_3 (puriss., >99.5%, Fluka, Buchs, Switzerland). The oxide was mixed with an equal weight of teflonized carbon black (25 wt.% polytetrafluoroethylene (PTFE) and 75 wt.% acetylene black) and the mixture was pressed onto a platinum current collector.

Room temperature liquid molten salt electrolyte consisting of 56 wt.% $AlCl_3$, 41 wt.% 1-ethyl-3-methylimidazolium chloride (EMIC), and 3 wt.% $MgCl_2$ was used at 80 °C for the Mg^{2+} insertion. The EMIC and $AlCl_3$ were made and purified as described in Refs. [16,17]. Further insertion experiments were carried out at room temperature in a 'wet' Mg^{2+}-containing electrolyte of 1 M $Mg(ClO_4)_2$ in acetonitrile (AN) with 3 mol% H_2O. Background-current measurements for this electrolyte system were performed with a magnesium-free electrolyte using 1 M tetrabutylammonium perchlorate ($TBAClO_4$) in AN with 3 mol% of H_2O. As Li^+-containing organic electrolyte, a solution of 0.5 M $LiClO_4$ in propylene carbonate (PC) was used. The organic Na^+ electrolyte was a solution of 0.5 M $NaClO_4$ in PC. Both the Li^+ and the Na^+ electrolyte had a water content of less than 10 ppm as verified with a Metrohm Model 684 Karl Fischer coulombmeter.

In the organic electrolyte systems, metallic lithium, sodium or magnesium served as counter electrodes, respectively. The Li/Li^+, Na/Na^+ (+0.22 V versus Li/Li^+), and Ag/Ag^+ (+3.57 V versus Li/Li^+) couples were used as references in the corresponding electrolytes. Metallic aluminium was used as counter electrode in the molten salt system; the Al/Al^{3+} couple (about +1.4 V versus Li/Li^+) was taken as reference potential therein.

The preparation of the electrolytes, as well as the cell assembly, was carried out in argon-filled glove boxes with less than 5 ppm of water and oxygen.

The electrochemical measurements were performed with standard instrumentation. For cyclic voltammetry scan rates between 10 and 100 $\mu V\ s^{-1}$ were typically used. Galvanostatic cycling was accomplished with current densities between 0.075 and 0.15 mA cm^{-2}.

For ex situ X-ray photoelectronspectroscopy (XPS) analyses, the working electrode stabilized at the desired potential was removed from the cell under argon atmosphere, rinsed thoroughly with dry deoxygenated acetonitrile overnight, and then dried in the glove-box atmosphere for several days. Parts of the electrode were then fixed on a platinum sample holder with a conducting silver paste. The XPS measurements were performed using Mg Kα radiation (1253.6 eV) on a Kratos ES 300 electron spectrometer. The fixed analyser transmission (FAT) mode was chosen. The vacuum in the analysis chamber was always better than 2×10^{-9} torr. Depth profiles were obtained by sputtering with argon ions (4 keV, 12 mA cm^{-2}, angle of incidence 45°).

3. Results and discussion

It is possible to insert Li^+ and Na^+ ions in MoO_3 from dry organic electrolytes. Fig. 2 shows typical cyclic voltammetric curves obtained for the lithium insertion from the 0.5 M $LiClO_4$/PC electrolyte. The depicted current is normalized to the mass of the electroactive oxide for sake of easy comparison with other Figures. The voltammogram in Fig. 2 shows a reversible insertion/de-insertion process in a potential range between about 2.0 and 2.3 V versus Li/Li^+. An additional reduction process occurs only in the first cycle with a peak potential

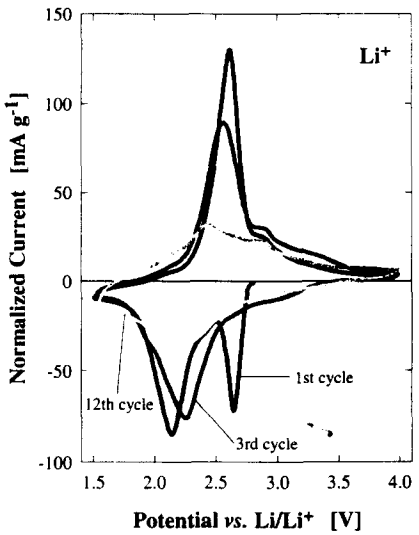

Fig. 2. Cyclic voltammogram of MoO_3 in 0.5 M $LiClO_4$/PC at 50 $\mu V\ s^{-1}$.

of about 2.7 V versus Li/Li^+. The shape of the peaks in the voltammogram changes with the increasing cycle number indicating a gradual structural change of the host material. A reduction charge of about 280 Ah kg^{-1} of the oxide is obtained in the first cycle.

The characteristics of molybdenum(VI) oxide as insertion electrode material in secondary, organic electrolyte lithium batteries concerning morphology, structural changes during cycling, and transport properties, have been well investigated [18,19]. During the initial reduction, a part of the inserted lithium is irreversibly trapped in the oxide, and $Li_{z+x}MoO_3$ is formed. In the following re-oxidation only x moles of lithium are deinserted and subsequently cycled. A complete lithium extraction seems to be hindered. The kinetically accessible stoichiometric range of the reversible lithium insertion/de-insertion is reported to be $0.1 < x < 1.5$ for Li_xMoO_3 [18]. Higher lithium uptake could only be achieved by serious structural rearrangements of the oxide which could not be observed on the experimental timescale at room temperature.

The insertion of lithium causes an increase of the interlayer distance because of the repulsion forces of the inserted cations. The interplanar distance is related to the lithium mobility and has a maximum for $x = 0.5$ [19]. This lattice expansion leads to cracking of the MoO_3 crystals during insertion and, thus, to a decrease in particle size [18]. As a result MoO_3 is cycled in a quasi-amorphous state. This explains why the voltammetric peaks change shape with increasing cycle number, whereas the specific charges obtained during cycling do not change dramatically. We obtained specific charges in these voltammetric measurements that are still 250 Ah kg^{-1} after 12 cycles. The significant decrease of the specific charge below 200 Ah kg^{-1} after 20 cycles can be interpreted as the crystallization of the electronically and ionically insulating Li_2MoO_4 phase from the quasi-amorphous electrode material that may lead to a partial passivation of the electrode, as suggested in Ref. [18].

Galvanostatic experiments, of which the first three cycles are shown in Fig. 3, lead to the same conclusions as the potentiodynamic measurements. The first discharge curve looks different from those following. At least two potential plateaus can be identified. The first plateau, observed at about 2.8 V versus Li/Li^+, corresponds to the generation of the lithium bronze Li_zMoO_3 with $0 < z < 0.3$. The subsequent reversible lithium insertion/de-insertion corresponds to the second plateau which appears at about 2.4 V versus Li/Li^+. The first galvanostatic cycle also verifies that Li_xMoO_3 cannot be regarded as a simple solid solution in the whole interval of $0 < x < 1.5$. At least two single phases exist in this stoichiometric range. An initial specific charge of about 300 Ah kg^{-1} could be obtained for the lithium insertion in the galvanostatic experiments with a current density of 0.15 mA cm^{-2}. This specific charge remains greater than 250 Ah kg^{-1} for 15 cycles and then decreases to 150 Ah kg^{-1} after 30 cycles as shown in Fig. 4.

The electrochemical insertion of sodium shows some similarities to that of lithium. A very sharp reduction peak found in the cyclic voltammogram at a potential of about 2.4 V versus Na/Na^+ in the first cycle (Fig. 5) indicates the formation of a sodium bronze, Na_zMoO_3. It is further reduced to $Na_{z+x}MoO_3$. Subsequently, x moles of sodium are cycled rather reversibly. The shape of the reduction peaks changes dramatically after the first cycle indicating a significant structural damage of the rather inflexible layered oxide, caused by the insertion of the much larger Na^+ cation. The increased ionic radius might also be the reason for the observed much slower insertion kinetics when compared to the Li^+ case. The galvanostatic experiments shown in Fig. 6 suggest the formation of the sodium bronze, Na_zMoO_3, with $0 < z < 0.4$ at a potential plateau of 2.5 V versus

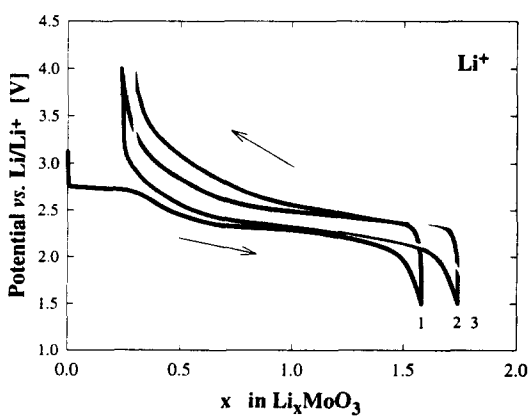

Fig. 3. Galvanostatic reduction and re-oxidation of MoO_3 in 0.5 M $LiClO_4$/PC at 0.15 mA cm^{-2} (first three cycles).

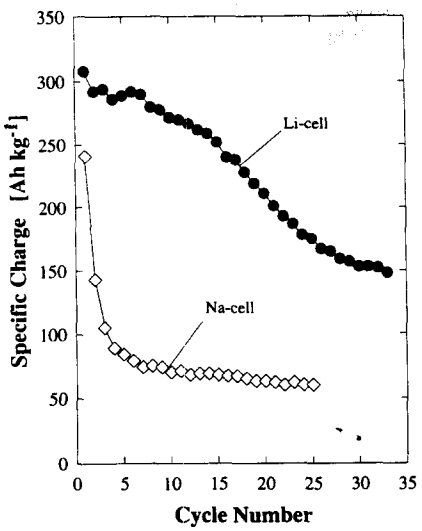

Fig. 4. Specific charge of MoO_3: (●) from galvanostatic cycling of the Li|0.5 M $LiClO_4$/PC|MoO_3 cell at 0.15 mA cm^{-2} as in Fig. 3, (◇) from galvanostatic cycling of the Na|0.5 M $NaClO_4$/PC|MoO_3 cell at 0.08 mA cm^{-2} as in Fig. 6.

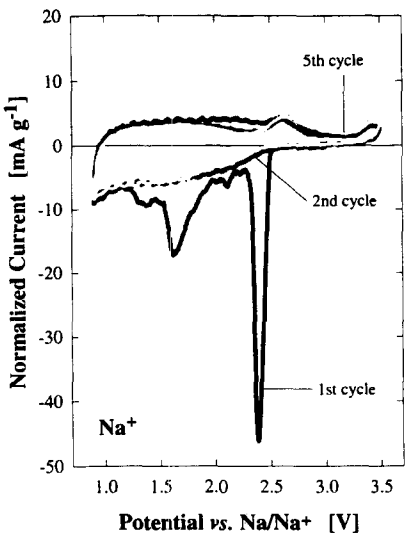

Fig. 5. Cyclic voltammogram of MoO_3 in 0.5 M $NaClO_4$/PC at 20 μmV s^{-1}.

Na/Na$^+$. A second plateau can be observed at about 1.8 V versus Na/Na$^+$. A maximum sodium uptake of about 1.5 moles is obtained at a potential limit of 1 V versus Na/Na$^+$. The re-oxidation to the sodium-free MoO_3 cannot be achieved; even more sodium is trapped in the oxide with subsequent cycling for kinetic reasons and, therefore, the available specific charge decreases. The initial specific charge for the Na$^+$ insertion from the galvanostatic experiments is about 240 Ah kg^{-1}. The available charge decreases rapidly and falls below 100 Ah kg^{-1} after three cycles (Fig. 4).

A significant electrochemical insertion of magnesium from dry, PC-based electrolytes was not observed. However, magnesium insertion could be achieved in room temperature liquid molten salt mixtures based on $AlCl_3$.

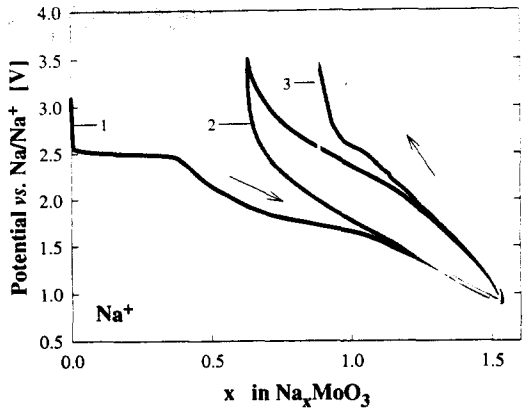

Fig. 6. Galvanostatic reduction and re-oxidation of MoO_3 in 0.5 M $NaClO_4$/PC at 0.15 mA cm^{-2} (first three cycles).

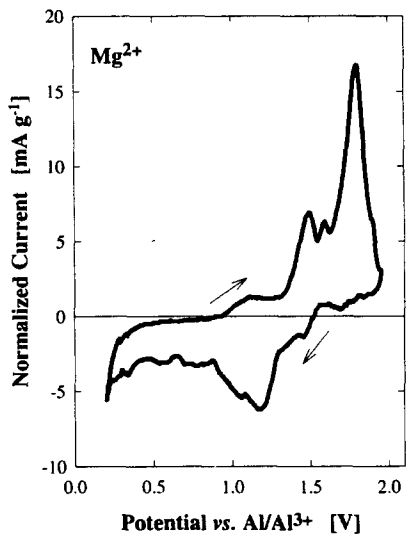

Fig. 7. Cyclic voltammogram of MoO_3 in 3 wt.% $MgCl_2$/41 wt.% EMIC/56 wt.% $AlCl_3$ at 10 μV s^{-1} (first cycle).

The acidic molten salt mixture of 40 mol% EMIC and 60 mol% $AlCl_3$ offers the possibility of overcoming essential problems related with magnesium-containing electrolyte solutions based on magnesium salts dissolved in pure organic solvents. The high polarization effect of the small and divalent Mg^{2+} cation causes poor solubility of many magnesium salts in organic solvents as well as a small degree of dissociation of the dissolved ion-pairs leading to a rather poor conductivity of the appropriate electrolytes. In the molten salt system up to 5 mol% $MgCl_2$ can be dissolved. Thus, the salt melt delivers a rigorously dry environment for the electrochemical Mg^{2+} insertion.

The magnesium insertion at 80 °C from the $MgCl_2$/EMIC/$AlCl_3$ molten salt electrolyte system is demonstrated in the cyclic voltammogram shown in Fig. 7. Obviously, it is possible to electrochemically insert/de-insert Mg^{2+} in MoO_3 reversibly according to an overall electrode reaction scheme:

$$MoO_3 + xMg^{2+} + 2xe^- \longleftrightarrow Mg_xMoO_3 \quad (2)$$

The electrochemical cycling of MoO_3 proceeds in the potential range from +0.7 to +1.95 V versus Al/Al^{3+}. In the first voltammetric reduction, specific charges of up to 160 Ah kg^{-1} of the oxide can be obtained with a scan rate of 10 $\mu V\ s^{-1}$. The complex fine structure of both the potentiodynamic and the galvanostatic curves (Figs. 7 and 8) indicate complicated structural changes of the oxide. In the initial galvanostatic discharge curve a specific charge of about 150 Ah kg^{-1} is reached which corresponds to about 0.76 electrons per one molybdenum atom in the MoO_3. However, the specific charge decreases gradually with the cycle number (Fig. 9) and falls below 100 Ah kg^{-1} after the fourth cycle.

The Mg^{2+} insertion can be enhanced using a 'wet' electrolyte. A cyclic voltammogram of MoO_3 in 1 M $Mg(ClO_4)_2$/AN with 3 mol% of H_2O is shown in Fig. 10. Specific charges of about 210 Ah kg^{-1} were achieved

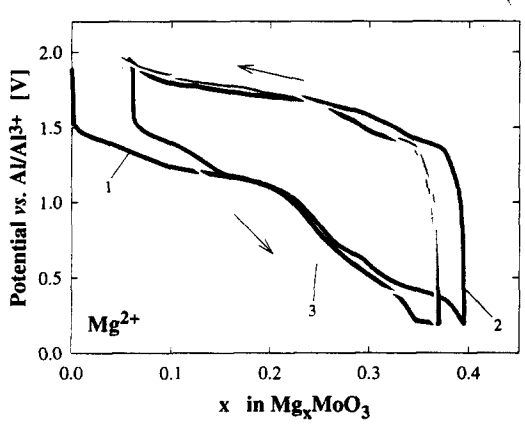

Fig. 8. Galvanostatic reduction and re-oxidation of MoO_3 in 3 wt.% $MgCl_2$/41 wt.% EMIC/56 wt.% $AlCl_3$ at 0.08 mA cm^{-2} (first three cycles).

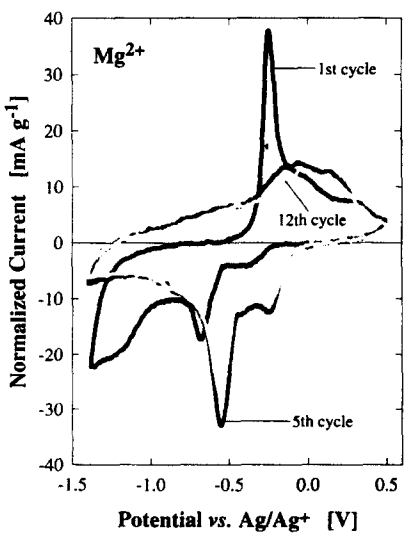

Fig. 9. Specific charge of MoO_3 obtained for the magnesium systems: (◇) the $MgCl_2$/EMIC/$AlCl_3$ salt melt, cycling as in Fig. 8, and (●) 1 M $Mg(ClO_4)_2$/AN with 3 mol% H_2O, cycling as in Fig. 10.

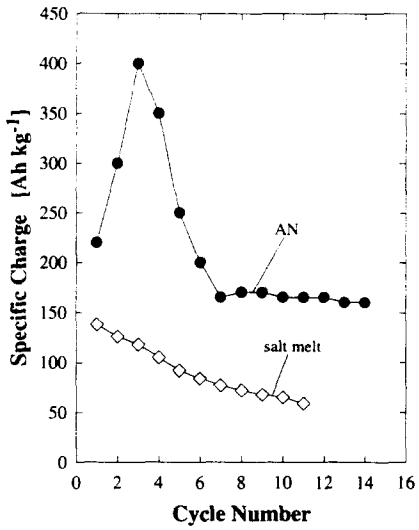

Fig. 10. Cyclic voltammogram of MoO_3 in the 'wet' 1 M $Mg(ClO_4)_2$/AN (3 mol% H_2O) electrolyte at 20 $\mu V\ s^{-1}$.

with a scan rate of 20 $\mu V\ s^{-1}$. The results on MoO_3 are consistent with those reported for the Mg^{2+} insertion in V_2O_5 and V_6O_{13} in which a strong dependence on the solvent and its water content was found [6,7]. One possible explanation for the effect of water could be the strong polarization effect of the small divalent Mg^{2+} cation which is strongly attenuated by solvating it with strong donor molecules such as H_2O. An enhancement effect on the magnesium-insertion process can also be observed if an electroactive material such as $NaV_3O_8(H_2O)_y$ contains the H_2O molecules in the form of lattice water in the crystal structure [1] [20].

Of course, the possibility of inserting H^+ parallel to Mg^{2+} from 'wet' electrolytes cannot be excluded. Background experiments have been attempted with the Mg^{2+}-free electrolyte, 1 M $TBAClO_4$ in AN with 3 mol% H_2O, and a stainless-steel counter electrode. They gave a specific charge of about 300 Ah kg^{-1} for the first reduction cycle. However, XPS measurements of the N:Mo ratio showed that high amounts of tetrabutylammonium cations could be inserted. Our insertion experiments performed with V_6O_{13} showed that the number of inserted protons from the 'wet' $Mg(ClO_4)_2$/AN electrolyte did not exceed 20% of the total charge [7]. A similar contribution of H^+ to the insertion process might also be expected for the case of the MoO_3.

4. Conclusions

As a first step towards novel rechargeable magnesium battery systems we have demonstrated the feasibility

[1] Results on the Mg^{2+} insertion in hydrated, layered vanadium bronzes, LiV_3O_8, NaV_3O_8, KV_3O_8, $Mg(V_3O_8)_2$, and $Ca(V_3O_8)_2$, are reported in another communication published in this volume [20].

of the electrochemical reduction, re-oxidation, and cycling of molybdenum(VI) oxide in dry, Mg^{2+}-containing electrolytes.

Acknowledgements

The XPS measurements performed by B. Schnyder, PSI, as well as the technical assistance of W. Scheifele, PSI, are gratefully acknowledged. We also thank the BEW (Swiss Federal Department of Energy) for financial support (Grant No. EF-PROCC(91)18).

References

[1] P.G. Bruce, F. Krok, J. Nowinski, V.C. Gibson and K. Tavakkoli, *J. Mater. Chem., 1* (1991) 705–706.
[2] J.P. Pereira-Ramos, R. Messina and J. Perichon, *J. Electroanal. Chem., 218* (1987) 241–249.
[3] R.J. Hoffman, R.C. Winterton and T.D. Gregory, *US Patent No. 4 894 302* (1990).
[4] T.D. Gregory, R.J. Hoffman and R.C. Winterton, *J. Electrochem. Soc., 137* (1990) 775–780.
[5] R.E. Dueber, J.M. Fleetwood and P.G. Dickens, *Solid State Ionics, 50* (1990) 329–337.
[6] P. Novák and J. Desilvestro, *J. Electrochem. Soc., 140* (1993) 140–144.
[7] F. Joho, P. Novák, O. Haas and R. Nesper, *Chimia, 47* (1993) 288.
[8] P. Novák, W. Scheifele and O. Haas, *Molten Salt Forum, 1–2* (1993/94) 389–396.
[9] P. Novák, V. Shklover and R. Nesper, *Z. Phys. Chem., 185* (1993) 51–68.
[10] L. Campanella and G. Pistoia, *J. Electrochem. Soc., 118* (1971) 1905–1908.
[11] P.G. Dickens and G.J. Reynolds, in C.H.F. Barry and P.C.H. Mitchell (eds.), *Proc. Climax Molybdenum, 4th Int. Conf. on Chemistry and Uses of Molybdenum*, Climax Molybdenum Co., Ann Arbor, MI, USA, 1982, p. 32.
[12] T. Ohzuku, in G. Pistoia (ed.), *Lithium Batteries*, Elsevier, Amsterdam, 1994, p. 256.
[13] C.-G. Granqvist, *Appl. Phys. A, 57* (1993) 3–12.
[14] J.O. Besenhard and R. Schöllhorn, *J. Power Sources, 1* (1976/77) 267–276.
[15] L. Kihlborg, *Ark. Kemi, 21* (1963) 357–364.
[16] Anonymous, The preparation of melt: 1-methyl-3-ethylimidazolium chloride plus aluminum chloride, *F.J. Seiler Technical Memorandum, FJSRL-TM-83-0016*, 1983.
[17] J. Desilvestro, F. Holzer, S. Müller and O. Haas, Aluminiumbatterien, *PSI Technical Rep. No. 94*, Villigen, Switzerland, 1991.
[18] J.O. Besenhard, J. Heydecke and H.P. Fritz, *Solid State Ionics, 6* (1982) 215–224.
[19] J.O. Besenhard, J. Heydecke, E. Wudy and H.P. Fritz, *Solid State Ionics, 8* (1983) 61–71.
[20] P. Novák, W. Scheifele and O. Haas, *J. Power Sources, 54* (1995) 479.